Sc3N@(C80-Ih(7))(CF3)14 and Sc3N@(C80-Ih(7))(CF3)16. Endohedral Metallofullerene Derivatives with Exohedral Addends on Four and Eight Triple-Hexagon Junctions. Does the Sc3N Cluste...

ARTICLE *in* JOURNAL OF THE AMERICAN CHEMICAL SOCIETY · NOVEMBER 2009

Impact Factor: 12.11 · DOI: 10.1021/ja9069216 · Source: PubMed

$Sc_3N@(C_{80}\text{-}I_h(7))(CF_3)_{14}$ and $Sc_3N@(C_{80}\text{-}I_h(7))(CF_3)_{16}$. Endohedral Metallofullerene Derivatives with Exohedral Addends on Four and Eight Triple-Hexagon Junctions. Does the Sc_3N Cluster Control the Addition Pattern or Vice Versa?

Natalia B. Shustova,[‡] Yu-Sheng Chen,[§,*] Mary A. Mackey,[¶] Curtis E. Coumbe,[¶] J. Paige Phillips,[¶,*] Steven Stevenson,[¶,*] Alexey A. Popov,[†,*] Olga V. Boltalina,[‡,*] and Steven H. Strauss[‡,*]

Contribution from Department of Chemistry, Colorado State University, Fort Collins, CO 80523, ChemMatCARS Beam Line, University of Chicago Advanced Photon Source, Argonne, IL 60439, Department of Chemistry and Biochemistry, University of Southern Mississippi, Hattiesburg, MS 39406, and Department of Electrochemistry and Conducting Polymers, Leibniz Institute for Solid State and Materials Research, Dresden D01069 Germany

RECEIVED DATE: ; yschen@cars.uchicago.edu; janice.phillips@usm.edu; steven.stevenson@usm.edu; a.popov@ifw-dresden.de; olga.boltalina@colostate.edu; steven.strauss@colostate.edu

[‡] Colorado State University

[§] University of Chicago Advanced Photo Source

[¶] University of Southern Mississippi

[†] Leibniz Institute for Solid State and Materials Research

Abstract

The compounds $Sc_3N@(C_{80}\text{-}I_h(7))(CF_3)_{14}$ (**1**) and $Sc_3N@(C_{80}\text{-}I_h(7))(CF_3)_{16}$ (**2**) were prepared by heating $Sc_3N@C_{80}\text{-}I_h(7)$ and $Ag(CF_3CO_2)$ to 350 °C in a sealed tube. The structures of **1** and **2** were determined by single-crystal X-ray diffraction. They are the first X-ray structures of any endohedral metallofullerene with more than four cage $C(sp^3)$ atoms. The structures exhibit several unprecedented features for metallic nitride fullerenes, including multiple cage sp^3 triple-hexagon junctions (four on **1** and eight on **2**), no cage disorder and little (**2**) or no (**1**) endohedral atom disorder, high-precision (C–C esd's are 0.005 Å for **1** and 0.002 Å for **2**), an isolated aromatic $C(sp^2)_6$ hexagon on **2**, and two negatively-charged isolated aromatic $C(sp^2)_5^-$ pentagons on **2** that are bonded to one of the Sc atoms. DFT calculations are in excellent agreement with the two Sc_3N conformations observed for **2** (ΔE(calc) = 0.36 kJ mol^{-1}; ΔE(exp) = 0.26(2) kJ mol^{-1}).

Introduction

Metallic nitride fullerenes (MNFs),[1,2] which are a subset of endohedral metallofullerenes (EMFs), have been the focus of intense research for the past decade.[3] This is in part because (i) they possess unusual structures[1,2,4,5] and physicochemical properties,[6] (ii) exohedral derivatives of them may find use in medical applications such as MRI and as X-ray contrast agents,[7,8] and (iii) recent breakthroughs in their synthesis and purification have made them available in larger quantities.[9-12] In 2007, we reported the synthesis and spectroscopic/electrochemical characterization of $Sc_3N@(C_{80}\text{-}I_h(7))(CF_3)_2$.[13] In this paper we report the synthesis and X-ray structures of two new derivatives with 14 and 16 CF_3 substituents,[14] $Sc_3N@(C_{80}\text{-}I_h(7))(CF_3)_{14}$ (**1**) and $Sc_3N@(C_{80}\text{-}I_h(7))(CF_3)_{16}$ (**2**) (hereinafter C_{80} will refer exclusively to the cage isomer $C_{80}\text{-}I_h(7)$[15]). These compounds and their molecular structures are significant for the following six reasons: **1** exhibits neither cage nor endohedral-atom disorder, a situation rarely observed in EMF X-ray structures[4,5] including the MNF $Sc_3N@C_{80}$[1,2] and its exohedral derivatives,[16-19] and **2** only exhibits a minor two-fold disorder of one Sc atom; they are the first X-ray structures of any EMF with more than four cage C(sp^3) atoms; they are rare examples of fullerene$(X)_n$ derivatives with one or more X groups on triple-hexagon junctions (i.e., with sp^3 THJs)[18,20-22] (**1** has four sp^3 THJs and **2** has eight of them); the addition pattern of **2** includes two isolated cyclopentadienyl(1−) rings; the structures are precise enough that a meaningful analysis of interatomic distances and angles can be performed and correlated with computational results at the DFT level of theory (the average estimated standard deviations (esd's) for cage C–C bond distances are 0.005 Å for **1** and 0.002 Å for **2**); the Sc_3N clusters in **1** and **2** are more distorted from three-fold symmetry than in any other MNF X-ray structure published to date, and the distortions are clearly caused by the pattern of cage C(sp^3) atoms in these compounds.

Results and Discussion

Compounds **1** and **2** were prepared and purified using methods we previously used for other trifluoromethylfullerenes such as $C_{60}(CF_3)_{2,4,6}$[23,24] $C_{70}(CF_3)_{2,4,6,8}$,[25] and Y@((C_{82}-$C_{2v}(9)$)$(CF_3)_5$).[26] Atmospheric-pressure photoionisation (APPI) mass spectra are shown in Figure S-1. In addition to **1** and **2**, other $Sc_3N@C_{80}(CF_3)_n$ compounds have been isolated using this synthetic method, and these will be reported in a separate paper once they have been more completely characterized. The HPLC purification scheme for **1** and **2** is shown in Figure S-2. The amounts of **1** and **2** that have been collected at this time are insufficient for detailed spectroscopic or electrochemical characterization. These two compounds are much less abundant than other isomers of $Sc_3N@C_{80}(CF_3)_{14}$ and $Sc_3N@C_{80}(CF_3)_{16}$, but the more abundant isomers have not yet been purified as well as **1** and **2**. However, the electrochemical behavior of $Sc_3N@C_{80}(CF_3)_2$ was studied previously, and it was found that it was 0.1 V easier to reduce than the parent MNF $Sc_3N@C_{80}$. Therefore, studying the electronic properties of the more abundant isomers will be an important part of our ongoing study of $Sc_3N@C_{80}(CF_3)_n$ derivatives.

Single crystals of **1** and **2** were studied by X-ray crystallography. Selected experimental parameters are listed in Table 1. The C_1 molecular structure of **1** and the idealized C_2 structure of **2** are shown in Figures 1 and 2, respectively (see S.I. for complete thermal ellipsoid plots and atom numberings). Numbered Schlegel diagrams for **1** and **2** are shown in Figure 3. The locants shown for **1** in Figures 1 and 3 are IUPAC lowest locants;[14] the same numbering scheme was adopted for **2** to facilitate comparisons with the structure of **1**. Selected interatomic distances and angles are listed in Table 2 along with relevant results for DFT-optimized $Sc_3N@C_{80}$, the numbering for which was also chosen to facilitate comparisons. To validate the DFT code that we used to optimize the structures of EMFs, plots showing the excellent agreement of X-ray vs. DFT-predicted cage C–C distances for **2** and the X-ray vs. DFT-predicted Sc–C and Sc–N distances for **1** and **2** are shown in Figure 4.

The CF_3 groups in **1** are attached to 14 cage C(sp^3) atoms that form a continuous ribbon of edge-sharing *para*- and *meta*-$C_6(CF_3)_2$ hexagons and 1,3-$C_5(CF_3)_2$ pentagons (each shared

edge is a cage C(sp^3)–C(sp^2) bond). Four CF_3 groups, on C1, C3, C17, and C65, exhibit two-fold rotational disorder (not shown in Figure 1). The C1, C3, and C17 CF_3 groups are ca. 50% staggered and ca. 50% eclipsed with respect to the three cage C–C bonds that radiate from the cage C atom to which they are attached, and the C65 CF_3 group is 88.6(4)% staggered and 11.4(4)% eclipsed. Ignoring these disordered CF_3 groups, the range of F···F contacts shorter than 3 Å between CF_3 groups that share the same hexagon or pentagon is 2.591(5)–2.791(5) Å. This range is normal for CF_3 derivatives of hollow higher fullerenes.[27-29]

The endohedral Sc_3N cluster in **1**, which formally has a 6+ charge,[30-32] is "locked" into position (i.e., it is not disordered), a situation that is rarely observed in MNFs (but is not unprecedented[4,21]). Addition of the 14 CF_3 groups undoubtedly results in electron-rich and electron-poor regions of the remaining fullerene π system when compared with $Sc_3N@C_{80}$. This effect, and the lack of any element of symmetry, apparently combine to make the observed orientation of the Sc_3N cluster in **1** more stable than alternative orientations, in sharp contrast to the situation in underivatized $Sc_3N@C_{80}$, in which the Sc_3N cluster exhibits rapid rotational averaging over many symmetry-equivalent orientations.[30,31,33-35] Similar conclusions about observed or proposed metal-atom localization in derivatized EMFs have been reached previously by us and by others,[13,19,36,37] but as far as X-ray structures are concerned, all previous examples have only two or four cage C(sp^3) atoms.[21] With the structures of **1** and **2** unambiguously determined, it is now possible to study in detail (i) the effect that addition patterns have on the experimentally-verified orientation of the Sc_3N cluster in highly-derivatized $Sc_3N@C_{80}$ compounds in particular and (ii) the role that addition patterns might play in orienting M_3N clusters in MNFs with multiple cage C(sp^3) atoms in general.

Four of the CF_3 groups in **1** are attached to C_{80} THJs C41, C45, C62, and C65. This is unprecedented. Before this work, no fullerene derivative of any kind had been found with more than two sp^3 THJs, probably because (i) sp^2 THJs are the least pyramidal cage C atoms in empty underivatized higher fullerenes,[38] and the release of angle strain at more pyramidal sites is part of the driving force for exohedral functionalization at those particular sites,[39] and (ii) no EMF with

more than four cage C(sp^3) atoms had been structurally characterized. However, the degree-of-pyramidalization in underivatized EMFs is more complicated than in empty underivatized higher fullerenes because some EMF sp^2 THJs are more pyramidal than some of the cage C(sp^2) atoms that make up the EMF pentagons (see S.I. for more information about pyramidalization in fullerenes). There are X-ray structures of two cycloadducts of MNFs that have one sp^3 THJ each, $Sc_3N@(C_{78}$-$D_{3h}(5))((CH_2)_2NCPh_3)$[21] and $Sc_3N@C_{80}((CH_2)_2NCPh_3)$.[18] The former compound appears to be the stable isomer of this composition; the latter compound isomerizes in solution to a more stable isomer with no sp^3 THJs.[18] In addition, the bis-cycloadduct $Sc_3N@(C_{78}$-$D_{3h}(5))(C(CO_2Et)_2)_2$ is believed to have two sp^3 THJs.[37]

Our DFT calculations, summarized in Figure 5, show that the 1,3,7,17,28,39,-41,45,47,51,54,62,65,70 isomer **1**, with four sp^3 THJs, is more stable than several hypothetical isomers without sp^3 THJs, viz. isomers 3, 5, 7, and 8. However, if the Sc_3N^{6+} cluster is removed from **1**, the remaining hexaanion 1,3,7,17,28,39,41,45,47,51,54,62,65,70-$C_{80}(CF_3)_{14}^{6-}$ is far less stable than $C_{80}(CF_3)_{14}^{6-}$ isomers 3 and 5. Therefore, the presence of the metal cluster appears to stabilize the formation of the four sp^3 THJs in **1**. We believe this is because the formation of sp^3 THJs tends to localize negative charge in pentagons to which one or more metal atoms are bonded. For example, the four sp^3 THJs in **1** are bonded to a common pentagon (see Figures 1 and 3), and this is the same pentagon that interacts strongly with Sc2 through C43 (see Table 2), the closest cage C atom to Sc2, and C42 and C44, the third and fourth closest cage C atoms to Sc2 (Sc2–C42 = 2.408(4) Å and Sc2–C44 = 2.408(3) Å). The evidence that this pentagon has become more "electron-rich" relative to the same pentagon in the precursor $Sc_3N@C_{80}$ is two-fold: (i) the C42–C63, C44–C63, and C63–C64 distances in **1** are ca. 1.41 Å whereas they are ca. 1.44 Å in (DFT-optimized) $Sc_3N@C_{80}$ (see Figure S-4); and (ii) Sc2 has moved from being closest to C23 and C24 in $Sc_3N@C_{80}$ to being closest to C22 and C43 in **1**, even though this has caused the Sc1–N–Sc2 bond angle to undergo a significant distortion from 120° in $Sc_3N@C_{80}$ to 136.7(1)° in **1**. In addition, note that sp^3 THJs C62 and C65 are also bonded to the pentagon that

interacts with Sc3, and C–C distances within that pentagon have also been shortened relative to $Sc_3N@C_{80}$ (see Figure S-4).

The CF_3 groups in **2**, none of which is disordered, are attached to 16 cage C(sp^3) atoms, half of which are sp^3 THJs (C34, C53, C57, C62, C65, C68, C71, and C74). (The range of F···F distances for **2** is 2.527(2)–2.900(2) Å.) In this compound, the localization of negative charge in pentagons reaches the maximum extent. The eight sp^3 THJs form a double loop of edge-sharing *p*-$C_6(CF_3)_2$ hexagons, and each loop of five *p*-$C_6(CF_3)_2$ hexagons surrounds an isolated pentagon composed of C(sp^2) atoms (i.e., the pentagons are isolated in that their π systems are not in conjugation with the rest of the fullerene π system or with each other; the *p*-$C_6(CF_3)_2$ hexagon that includes C71 and C74 is common to both loops). Isolated $C(sp^2)_5^-$ pentagons with *six* π electrons in fullerene derivatives (i.e., in $C_{60}X_5^-$ anionic moieties) are aromatic and can coordinate to *exohedral* metal atoms in η^5 Cp-like fashion.[40] However, in **2** the isolated pentagons coordinate to an *endohedral* metal atom, Sc3.

Formally, each isolated pentagon has received one of the two electrons that Sc3 donates to the C_{80} cage to become a six-electron aromatic $C(sp^2)_5^-$ pentagon. The Sc3 atom appears to be η^2 bonded to both isolated pentagons simultaneously, although not equally, and this inequality leads to the observed disorder in the position of Sc3 (see Table 2; Sc3a (43(2)% occupancy and Sc3b (57(2)% occupancy) are 0.455(3) Å apart). In the structure of $Sc(\eta^5\text{-}Cp^*)_2(CH_2CMe_3)$, the ranges of Sc–C(Cp) and C(Cp*)–C(Cp*) distances are 2.482(4)–2.541(4) Å and 1.403(5)–1.423(5) Å, respectively.[41] In **2**, the ranges of Sc3a/b–C and C–C distances involving the isolated pentagons are 2.20(5)–2.92(9) Å and 1.401(2)–1.441(2) Å, respectively (the longest C–C bond in each of the isolated $C(sp^2)_5^-$ pentagon is the one that is closest to Sc3, C72–C73 and C76–C80; note that the range of all C(sp^2)–C(sp^2) distances in **2** is 1.344(2)–1.470(2) Å). Another indication of the aromatic, electron-rich nature of the isolated pentagons is that C72–C73 and C76–C80 are significantly shorter than C13–C31 (1.461(2) Å and C42–C43 (1.459(2) Å), which are η^2 bonded to Sc1 and Sc2, respectively, and are not part of isolated aromatic $C(sp^2)_5^-$ pentagons (see Figure S-5). Interestingly, the distances between Sc3a or Sc3b and the centroids

of their respective isolated pentagons are ca. 2.28 Å, only 0.07 Å longer than the corresponding distances in $Sc(\eta^5\text{-}Cp^*)_2(CH_2CMe_3)$ (ca. 2.21 Å).[41]

In harmony with the X-ray structure of **2**, our DFT calculations show that there are two conformational isomers of **2** that differ only in the position of Sc3 (the calculated Sc3a···Sc3b distance is 0.457 Å). The predicted energy difference between these conformers is 0.78 kJ mol^{-1} and is reduced to 0.36 kJ mol^{-1} if zero-point vibrational energy (ZPVE) is taken into account. We also located the transition state between the conformers, and found it to be only 1.36 kJ mol^{-1} above the lower energy structure (0.69 kJ mol^{-1} if ZPVE is also considered; to ensure that this transition state corresponds to the true energy barrier between the conformers, intrinsic-reaction-coordinate calculations were carried out following the normal mode with an imaginary frequency in both directions). With such a low energy barrier to interconversion, the disorder found in the position of Sc3 is almost certainly a true equilibrium at 100 K, the temperature of the X-ray data collection. An equilibrium quotient of 1.3(1) can be calculated for the conformational equilibrium {Sc3a-conformer} $\rightleftharpoons$ {Sc3b-conformer} (i.e., 57(2) ÷ 43(2) = 1.3(1)). At 100 K, this corresponds to an energy difference of 0.26(2) kJ mol^{-1}, in excellent agreement with the DFT predicted value of 0.36 kJ mol^{-1}. This is the first time that an experimentally observed disorder in M_3N cluster conformations in an MNF has been shown by theory to be due to two or more energy minima, each with a full set of non-imaginary frequencies, and that the transition between the minima has a low barrier.

The orientations of the Sc_3N cluster in **1**, **2**, and DFT-optimized $Sc_3N@C_{80}$ are quite similar. In all three cases C13 is the closest or second closest cage C atom to Sc1 and C76 and C80 are two of the closest cage C atoms to Sc3. It is Sc2 that appears to "move" the most in the three molecules, from the C23–C24 bond in $Sc_3N@C_{80}$ to the C22–C43 bond in **1** to the C42–C43 bond in **2**, and this causes the Sc1–N–Sc2 angle to increase from 120° in $Sc_3N@C_{80}$ to 136.7(1)° in **1** to 150.52(7)° in **2**. The distortion of the Sc_3N cluster in **2** from trigonal symmetry is larger than in any other observed MNF structure (one Sc–N–Sc angle was predicted to be 150°

in non-IPR $Sc_3N@C_{70}$;[42] the previously largest M–N–M angle in an MNF found by X-ray crystallography is 131.6(1)° in $Sc_3N@C_{80}$-$D_{5h}(6)$[4]).

A soon-to-be-published computational study of metal-cage bonding in EMFs reports that endohedral metal ions bond more strongly to sp^2 pentagon-hexagon-hexagon junctions (PHHJs) than to sp^2 THJs.[43] Since each metal ion is generally bonded to two or more cage C(sp^2) atoms, and since the addition patterns of fullerene$(R_f)_n$ compounds tend to be ribbons of edge-sharing *p*-C_6X_2 and *m*-C_6X_2 hexagons when $n \leq 12$ (generally with one R_f group per pentagon), there may be a competition between the endohedral metal ions and the exohedral R_f groups for the limited number of "suitable" sp^2 PHHJs. This may be an important part of the reason why, with 14 and 16 exohedral CF_3 groups, **1** and **2** have such an abundance of sp^3 THJs. In other words, if the Sc atoms must be closest to PHHJs, and if the CF_3 groups must lie on a ribbon, and if there are more than 12 CF_3 groups, then at least some low-energy MNF$(CF_3)_n$ isomers will have ribbons with sp^3 THJs.

Based on the experimental results in this paper and the aforementioned computational results, it now seems likely that multiple sp^3 THJs in MNFs, and possibly in EMFs in general, will be a common phenomenon when they are highly functionalized. (This will not be welcome news to fullerene theorists, who can no longer rely on THJs being unlikely sites for exohedral additions when deciding which isomers to study computationally.) Will it also be found, in general, that the metal atoms in such MNFs will be "drawn" to pentagons that are one bond removed from the sp^3 THJs (i.e., that M_3N cluster orientations and distortions will be determined by addition patterns, especially addition patterns that include sp^3 THJs)? The answer may be Yes. There is another example of this phenomenon in the literature, with a different fullerene cage. As mentioned above, the compound $Sc_3N@(C_{78}$-$D_{3h}(5))((CH_2)_2NCPh_3)$ has two adjacent cage C(sp^3) atoms, one of which is a THJ.[21] Drawings of two fragments of this molecule, shown in Figure 6, show that Sc1 is shifted toward the pentagon bonded to the sp^3 THJ, whereas Sc2 is almost exactly centered on its closest cage C–C bond. Furthermore, Sc3 is shifted toward a different pentagon that is also bonded to the sp^3 THJ (Sc1 and Sc3 are essentially, although not

crystallographically, symmetry related). The net result is that the Sc1–N–Sc3 angle in this compound, at 111.3(1)°,[21] is significantly smaller than the DFT-predicted angle of 120° in underivatized $Sc_3N@(C_{78}$-$D_{3h}(5))$.[44] (The Sc1–N–Sc2 and Sc2–N–Sc3 angles in the cycloadduct are 123.5(1) and 125.5(1), respectively[21]). It is possible that there is also a steric reason for the small Sc1–N–Sc3 angle in $Sc_3N@(C_{78}$-$D_{3h}(5))((CH_2)_2NCPh_3)$: the formation of cage $C(sp^3)$ atoms, in general, "enlarges" the fullerene cage in the vicinity of those atoms, and Sc1 and Sc3 might move towards one another because the cage is larger in the region between them. The compound $Sc_3N@(C_{78}$-$D_{3h}(5))(C(CO_2Et)_2)_2$ is believed to have two sp^3 THJs, one for each cycloadduct, and both of these were proposed to be connected to the pentagons bonded to Sc1 and Sc3.[34] According to our DFT optimization of a model for this compound, with CH_2 substituents replacing the two $C(CO_2Et)_2$ groups, the Sc1–N–Sc3 angle should be 110.6°. In other words, we predict that Sc1 and Sc3 in this compound are also drawn towards the more electron-rich pentagons, which in this case are each bonded to two sp^3 THJs.

Another interesting, and presumably stabilizing, feature of the structure of **2** is the presence of the isolated aromatic benzenoid ring comprising C1 and C5–C9. The bond distances within this ring, 1.398(2)–1.405(2) Å, are the same at the ±3σ level of confidence. For fullerene derivatives with more than 70 cage C atoms, this structural feature has also been observed in $C_{74}F_{38}$,[45] $C_{78}Br_{18}$,[46] $C_{78}Cl_{18}$,[47] and $C_{90}Cl_{32}$.[48] Figure 2 shows that this region of **2** is flattened relative to the rest of the cage. The average POAV angle, a measure of the departure from planarity for $C(sp^2)$ atoms (see S.I.),[15,49] is 5.7° for C1 and C5–C9, whereas it is 9.4° for the hexagon in **2** that includes C38 and C41 and it is 9.6° for the C1/C5–C9 hexagon in DFT-optimized $Sc_3N@C_{80}$ (for comparison, it is 11.6° for the $C(sp^2)$ atoms in C_{60}).

Finally, while it is obvious that the presence of the Sc_3N cluster has a strong influence on the pattern of CF_3 radical additions to $Sc_3N@C_{80}$, we have also shown that the addition pattern of exohedral substituents can have a strong influence on the geometry of the Sc_3N cluster in $Sc_3N@C_{80}X_n$ derivatives. The combination of (i) using endohedral metal clusters to direct the addition of exohedral substituents and (ii) using substituent addition patterns (which can be

modified by changing the substituent steric and/or electronic properties) to modify the geometry and hence the properties of endohedral metal clusters may allow the synthesis of technologically-useful, highly-derivatized, metal-cluster-containing EMFs in the near future.

Experimental Section

Synthesis and Purification of $Sc_3N@C_{80}(CF_3)_{14}$ and $Sc_3N@C_{80}(CF_3)_{16}$. All reagents and solvents were of the highest commercially-available purity and were used as received. The compound $Sc_3N@C_{80}$ was prepared as previously described.[9,10] In a typical synthesis, $Sc_3N@C_{80}$ (8.8 mg, 0.0079 mmol) and silver trifluoroacetate (AgTFA; 108 mg, 0.489 mmol) were ground together in a mortar and pestle. The mixture of solids was loaded into a 0.4 cm ID × 10.5 cm glass test tube, which was then sealed in a 0.6 cm ID × 11.5 cm copper tube with Swagelok fittings at both ends. The sealed reactor was heated at 350 °C for 2.5 h in a 8 cm ID × 45 cm long tube furnace. The product mixture was separated into the two title compounds by two-stage HPLC (10 mm ID × 250 mm Cosmosil Buckyprep column (Nacalai Tesque, Inc.); 300 nm UV detection). In the first stage, the eluent was 5 mL min^{-1} toluene. Both compounds were collected in a fraction that eluted between 2.9 and 8.0 min. In the second stage, the eluent was 5 mL min^{-1} heptane. The compound $Sc_3N@(C_{80})(CF_3)_{16}$ eluted first, at 10.5 min; $Sc_3N@C_{80}(CF_3)_{14}$ eluted at 15.0 min. The compounds exhibited molecular anions in atmospheric-pressure photoionisation (APPI) mass spectra at 2075.8 *m*/*z* for $Sc_3N@C_{80}(CF_3)_{14}$ (calc'd. 2075.8) and at 2213.8 *m*/*z* for $Sc_3N@C_{80}(CF_3)_{16}$ (calc'd. 2213.8), as shown in Figure S-1. An Agilent Technologies Model 6210 TOF spectrometer was used for these experiments, and an acetonitrile solution that contained 1% toluene was used for flow injection.

X-ray Crystallography. For both structures, absorption and other corrections were applied using SADABS. The structures were solved using direct methods and refined (on F^2, using all data) by a full-matrix, weighted least squares process. Standard Bruker control and integration software (APEX II) was employed, and Bruker SHELXTL software was used for structure solution, refinement, and graphics.

Crystals of $Sc_3N@C_{80}(CF_3)_{14}\cdot 0.5(C_8H_{10})$ (**1**) were grown by slow evaporation of a saturated *p*-xylene solution. Relevant experimental parameters are listed in Table 1. A diffraction-quality single crystal (0.014 × 0.062 × 0.074 mm) was mounted in paratone oil on a glass fiber glued to a small copper pin. X-ray diffraction data were collected at ChemMatCARS Sector 15-B at the Advanced Photon Source at Argonne National Laboratory (CARS = Consortium for Advanced Radiation Sources). The data set was collected at 100 K using a diamond (111) crystal monochromator, a wavelength of 0.4428 Å, and a Bruker CCD detector with 1 s counting per frame. Unit-cell parameters were refined by least squares using 9908 reflections. There is one molecule of $Sc_3N@C_{80}(CF_3)_{14}$ in the asymmetric unit; neither the carbon cage nor the Sc_3N cluster is disordered. Four of the CF_3 groups exhibit rotational disorder. The site-occupancy factors of the two modeled orientations for the trifluoromethyl groups that include C103, C104, C117, and C165 were 49/51%, 48/52%, 51/49%, and 89/11%, respectively. All of the F atoms in the major and minor disordered parts were refined anisotropically. A crystallographic information file is available in S.I.

Crystals of $Sc_3N@C_{80}(CF_3)_{16}$ (**2**) were grown by slow evaporation from saturated heptanes/toluene solution. Relevant experimental parameters are listed in Table 1. A diffraction-quality single crystal (0.040 × 0.040 × 0.060 mm) was mounted in paratone oil on a MiTeGen 10 μm loop. The data set was collected at 100 K using a silicon (111) crystal monochromator on a D8 goniostat equipped with a Bruker APEXII CCD detector at Beamline 11.3.1 at the Advanced Light Source at Lawrence Berkeley National Laboratory using synchrotron radiation tuned to λ=0.7749 Å. There is one molecule of $Sc_3N@C_{80}(CF_3)_{16}$ in the asymmetric unit; neither the carbon cage nor the CF_3 groups are disordered. One Sc atom in Sc_3N cluster is disordered among two positions, Sc3A and Sc3B, with site-occupancy factors 43(2)% and 57(2)%, respectively. The major and minor disordered parts of Sc3 atom were refined anisotropically. A crystallographic information file is available in S.I.

DFT calculations. All DFT calculations were performed using PBE functional[50] and TZ2P-quality basis set with SBK-type effective core potential for Sc atoms implemented in the

PRIRODA package.[51,52] The quantum-chemical code employed expansion of the electron density in an auxiliary basis set to accelerate evaluation of the Coulomb and exchange-correlation terms. Although the DFT-optimized structure of **1** could be directly compared to the X-ray-derived coordinates, the disorder found in **2** required a more complicated analysis. Our calculations showed that there are two conformational isomers of **2**, with different positions of Sc3. The other structural parameters of the conformers are very similar but are not identical. Hence, the X-ray-derived coordinates correspond to the average coordinates of the two conformers, and comparison of the experimental and DFT-optimized structural parameters should take this fact into account. In this regard, the DFT coordinates of **2** that we used to make the plot in Figure 4 are average DFT-optimised coordinates of the two conformers taken with weights corresponding to the X-ray determined occupancies of Sc3a and Sc3b. The DFT coordinates of the conformers used for the averaging were obtained using intrinsic-reaction-coordinate calculations. That is, we first optimized the structure of the transition state. Then, the normal coordinate corresponding to the imaginary frequency was followed in two directions until the energy minima were reached on each side of the barrier, and the coordinates of these minima were used for the averaging. This procedure ensures that coordinates of the conformers are different only in the displacement along the reaction coordinate and are not affected by translation or rotation of the molecules. It should be noted that the use of the DFT coordinates for either one of the conformers to construct a plot similar to the one in Figure 4 gives the same excellent correlation for the cage C–C bonds as use of the averaged coordinates. However, the DFT-predicted Sc–C distances for the averaged coordinates are in much better agreement with the corresponding X-ray values than the DFT-predicted Sc–C distances for either conformer alone.

Acknowledgment. We are pleased to acknowledge Lothar Dunsch for his encouragement and support and Simon Teat, Christine M. Beavers, Igor V. Kuvychko, and Ulrike Nitzsche for experimental and technical assistance. This work was supported by the Alexander von Humboldt Foundation (Fellowship to A.A.P.), the U.S. National Science Foundation (Grants CHE-

0707223, CHE-0547988, CHE-0847481, and DBI-0619455), the Civilian Research and Development Foundation (Grant RUC2-2830-MO-06), and the U.S. Department of Education (GAANN Fellowship Grant P200A060323). ChemMatCARS Sector 15 is principally supported by the National Science Foundation/Depart-ment of Energy under grant number CHE-0535644. Use of the Advanced Photon Source was supported by the U.S. Department of Energy, Office of Science, Office of Basic Energy Sciences, under Contract No. DE-AC02-06CH11357. We gratefully acknowledge the beam time obtained at the 11.3.1 beamline at the Advanced Light Source at Lawrence Berkeley National Laboratory, which is supported by the Director, Office of Science, Office of Basic Energy Sciences, of the U.S. Department of Energy under Contract No. DE-AC02-05CH11231.

Supporting Information Available: Crystallographic information files for **1** and **2**, additional figures of the structures of **1** and **2**, the HPLC purification of **1** and **2**, and APPI mass spectra of **1** and **2**. This material is available free of charge via the Internet at http://pubs.acs.org.

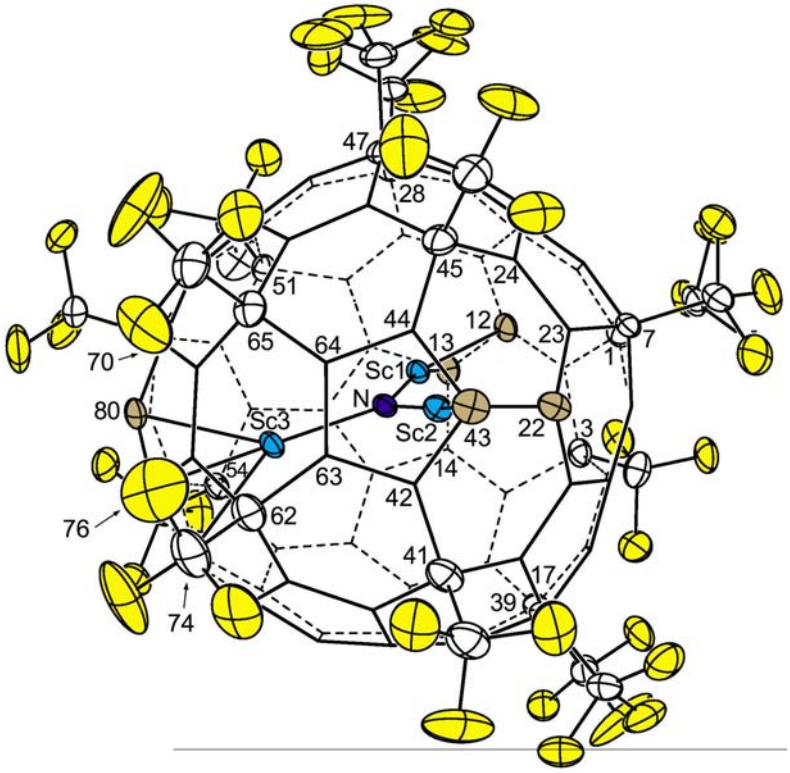

Figure 1. IUPAC-numbered thermal ellipsoid plot (TEP) of **1** (50% probability ellipsoids for F, N, Sc, and selected C atoms). The molecule is oriented to highlight the nearly-planar Sc_3N cluster, the light-brown cage C atoms to which the blue Sc atoms are attached, and the four CF_3 groups on the triple-hexagon junctions C41, C45, C62, and C65. The Sc_3 least squares plane (LSP) is tilted 77.0° from the C42-C63-C64-C44 LSP (the plane of the page for the TEP) and 88.6° from the C5-C6-C8-C9 LSP (the plane of the page for the Schlegel diagram). The unnumbered yellow ellipsoids are the 42 F atoms. Two of the three cage C atoms attached to Sc3, C74 and C76, are hidden from view, as is C70. The four CF_3 groups on C1, C3, C17, and C65 each exhibit a two-fold rotational disorder, but only one of the two orientations for these CF_3 groups are shown in the TEP.

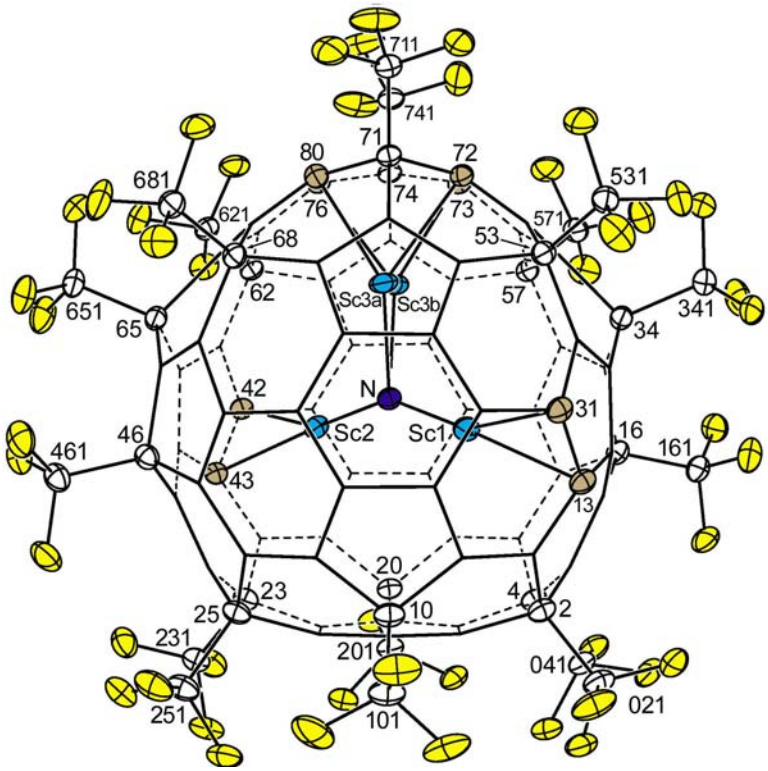

Figure 2. IUPAC-numbered thermal ellipsoid plot of **2** (50% probability ellipsoids for F, N, Sc and selected C atoms). The molecule, which has idealized but not crystallographic C_2 symmetry, is oriented to highlight the unusually large Sc1–N–Sc2 angle of 150.52(7)° (the molecular C_2 axis bisects this bond). The isolated benzenoid hexagon is at the bottom and the two isolated $C(sp^2)_5^-$ pentagons, which are joined by C71 and C74, are at the top. The unnumbered yellow ellipsoids are the 48 F atoms. The IUPAC locants shown are not the lowest set of locants; they are the same as those used for **1** to facilitate comparisons with **1**. The correct IUPAC lowest locants are given in Table 2.

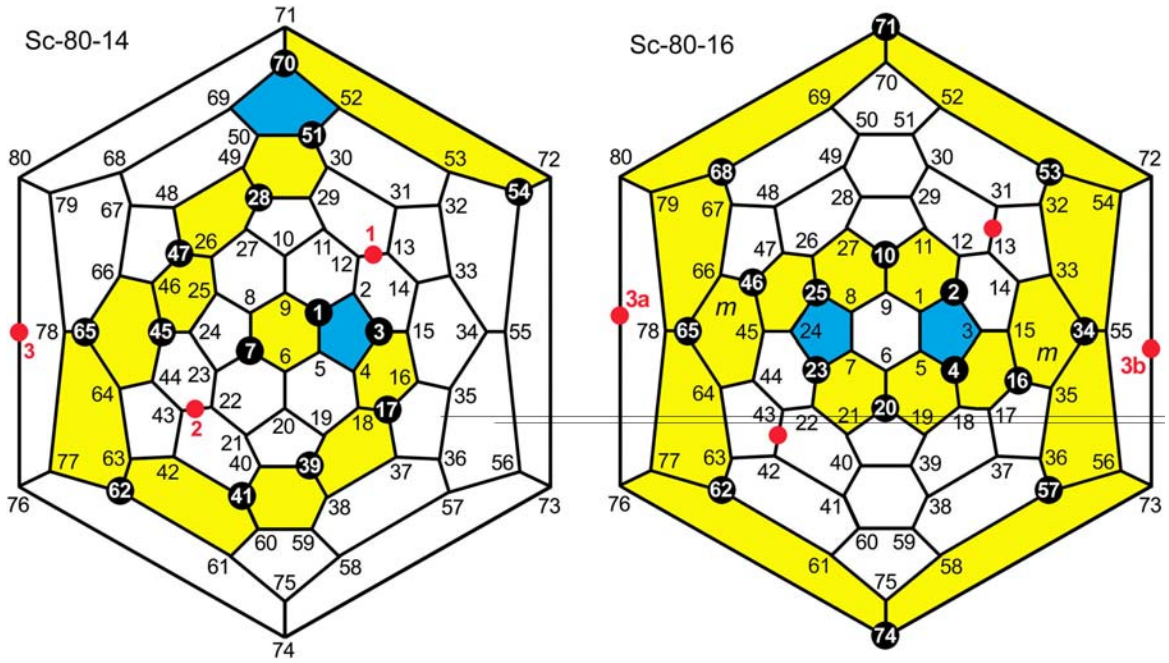

Figure 3. IUPAC-numbered Schlegel diagrams for **1** ($Sc_3N@C_{80}(CF_3)_{14}$, left) and **2** ($Sc_3N@C_{80}(CF_3)_{16}$, right). The black circles indicate the cage C(sp^3) atoms bonded to the CF_3 groups, *para*- and *meta*-$C_6(CF_3)_2$ hexagons are highlighted in yellow, 1,3-$C_5(CF_3)_2$ pentagons are highlighted in blue, and the Sc atoms are indicated by numbered red circles, which are placed on the C–C bonds of two cage C(sp^2) atoms closest to the Sc atoms (the ca. half-occupancy atoms Sc3a and Sc3b in **2** are also close to C73 and C76, respectively). In the DFT-optimized structure of $Sc_3N@C_{80}$, Sc1 is closest to C13 and C14, Sc2 is closest to C23 and C24, and Sc3 is closest to C76 and C80.

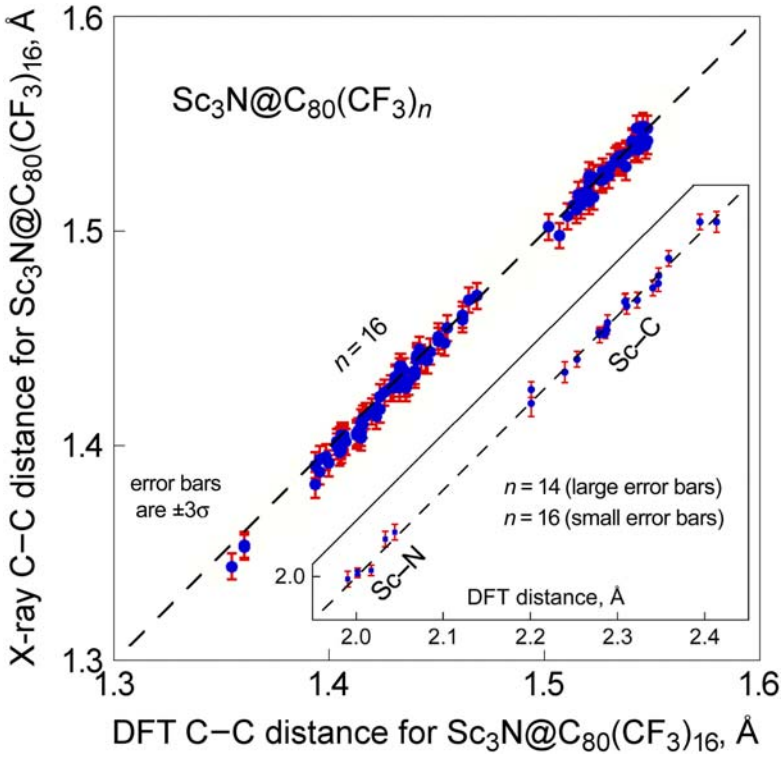

Figure 4. Comparison of the 120 X-ray and DFT-optimized cage C–C bonds in **2** and the Sc–C and Sc–N bonds in **1** and **2** (the error bars for the X-ray distances are ±3σ); the *x* and *y* axes for the smaller graph are identical to one another). The dashed lines have slope = 1 and pass through the origin. The four shortest X-ray cage C–C bonds in **2** are: C35–C36, 1.344(2) Å; C66–C67, 1.344(2) Å; C3–C15, 1.353(2) Å; and C24–C45, 1.354(2) Å. Several DFT vs. X-ray Sc···C distances greater than 2.35 Å are shown in the smaller graph but are not considered to be primary bonding interactions between the Sc atoms and the cage.

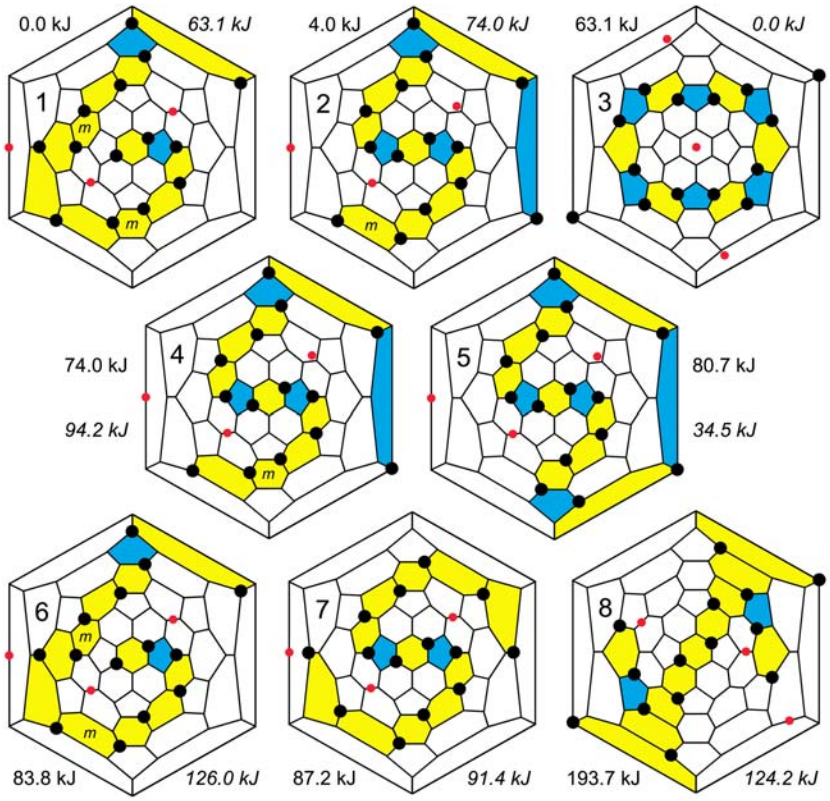

Figure 5. Schlegel diagrams for **1** (labelled **1**, upper left) and seven hypothetical isomers of $Sc_3N@C_{80}(CF_3)_{14}$. The black circles indicate the cage C(sp^3) atoms bonded to the CF_3 groups, *para*- and *meta*-$C_6(CF_3)_2$ hexagons are highlighted in yellow, 1,3-$C_5(CF_3)_2$ pentagons are highlighted in blue, and the Sc atoms are indicated by small red circles. DFT-predicted relative energies are shown for the compounds (regular font) and for the $C_{80}(CF_3)_{14}^{6-}$ hexaanions with the same addition pattern (italic font). Note that isomers 3, 5, 7, and 8 do not have sp^3 THJs.

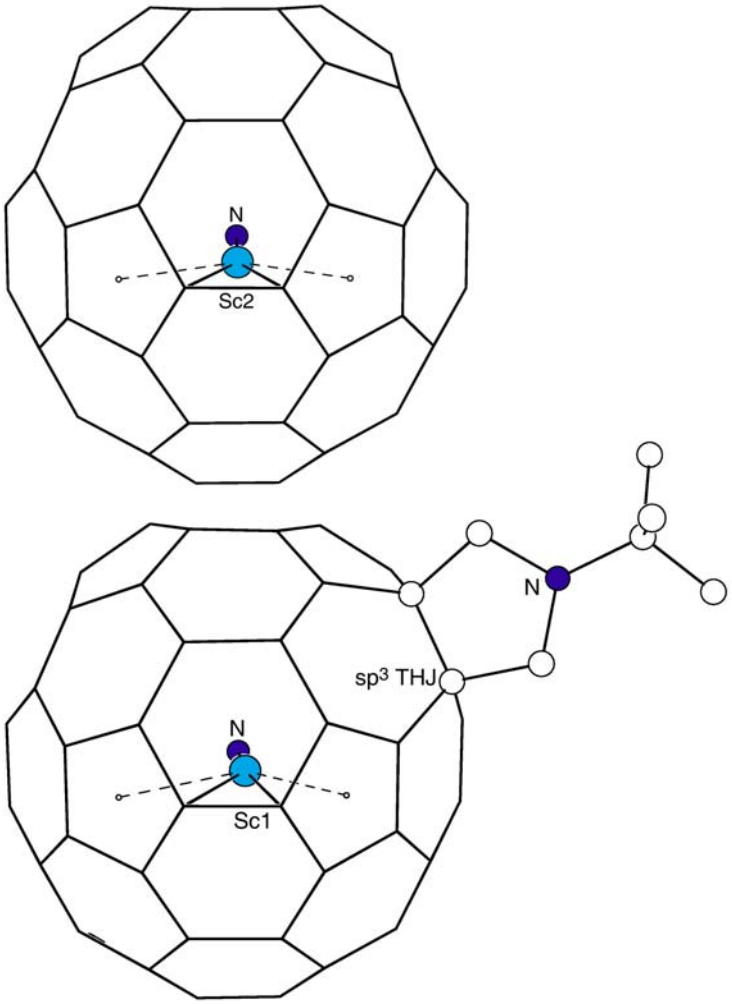

Figure 6. The X-ray structure of $Sc_3N@(C_{78}\text{-}D_{3h}(5))((CH_2)_2NCPh_3)$ was reported in ref. [21]. These drawings show that Sc1, unlike Sc2, is displaced from a position equidistant from its two closest cage C atoms towards the pentagon bonded to the sp^3 THJ. Since Sc3 is essentially (but not crystallographically) symmetry-related to Sc1, it is also displaced towards the sp^3 THJ in a similar way. The dashed lines connecting the Sc atoms to the centroids of the pentagons to which they are bonded are intended as visual aids and have no special significance. Only the *ipso* C atoms of the three phenyl groups are shown.

Table 1. Crystal data and structure refinement for $Sc_3N@C_{80}(CF_3)_{14}$ (**1**) and $Sc_3N@C_{80}(CF_3)_{16}$ (**2**)

compound	$Sc_3N@C_{80}(CF_3)_{14}\cdot 0.5\ C_8H_{10}$	$Sc_3N@C_{80}(CF_3)_{16}$
molecular formula, formula weight	$C_{94}F_{42}NSc_3\cdot 0.5(C_8H_{10})$, 2128.01 g mol^{-1}	$C_{96}F_{48}NSc_3$, 2213.85 g mol^{-1}
crystal system, space group, Z	monoclinic, $P2_1/n$, 4	triclinic, $P\bar{1}$, 2
color of crystal	brown	red
unit cell dimensions	a = 13.618(1) Å	a = 13.8756(6) Å
	b = 25.451(2) Å	b = 15.3985(7) Å
	c = 19.3451(16) Å	c = 16.7884(7) Å
	α = 90°	α = 73.911(3)°
	β = 98.491(2)°	β = 88.258(3)°
	γ = 90°	γ = 74.257(3)°
data collection temperature	100(2) K	100(2) K
final R indices, $R_1[I > 2\sigma(I)]$, wR_2 [all data]	0.0661, 0.1894	0.0437, 0.1253
goodness-of-fit on F^2	1.071	1.010

Table 2. Selected distances (Å) and angles (deg) for the Sc_3N moiety[a]

parameter	**1** (X-ray)	**2** (X-ray)	$Sc_3N@C_{80}$ (DFT)
Sc1–N	2.043(3)	2.0057(13)	2.034
Sc2–N	2.051(3)	2.0027(13)	2.034
Sc3a–N	1.997(3)	2.013(2)	2.034
Sc3b–N		2.007(2)	
Sc1–N–Sc2	136.7(1)	150.52(7)	120.0
Sc1–N–Sc3	120.3(1)	102.2(2); 107.3(1)[b]	120.0
Sc2–N–Sc3	102.9(1)	107.1(1); 102.1(1)[b]	120.0
Sc1–C	2.278(3) (C13)	2.2844(16) (C13)	2.294 (C13)
Sc1–C	2.318(3) (C12)	2.2806(15) (C31)	2.263 (C14)
Sc2–C	2.235(4) (C43)	2.2837(15) (C43)	2.263 (C23)
Sc2–C	2.311(3) (C22)	2.2784(15) (C42)	2.294 (C24)
Sc3(a)–C	2.250(3) (C76)	2.337(3) (C76)	2.263 (C76)
Sc3(a)–C	2.292(3) (C80)	2.199(5) (C80)	2.294 (C80)
Sc3(a)–C	2.332(3) (C74)	2.316(3) (C72)	2.388 (C73)
Sc3b–C		2.317(2) (C76)	
Sc3b–C		2.215(3) (C73)	
Sc3b–C		2.346(3) (C72)	
Sc3b–C		2.434(3) (C80)	

[a] All three compounds considered have the C_{80}-I_h(7) cage; compound **1** is $Sc_3N@$(1,3,7,17,28,-39,41,45,47,51,54,62,65,70-$C_{80}(CF_3)_{14}$) (IUPAC lowest locants); compound **2** is $Sc_3N@$(2,4,10,-16,20,23,25,34,46,53,57,62,65,68,71,74-$C_{80}(CF_3)_{16}$) using a locant set that facilitates comparisons with **1** (the IUPAC lowest locants for **2** are actually 1,3,7,13,17,21,30,39,42,49,53,62,65,-68,71,74). [b] The first value is for Sc3a and the second value is for Sc3b.

References

(1) Stevenson, S.; Rice, G.; Glass, T.; Harich, K.; Cromer, F.; Jordan, M. R.; Craft, J.; Hadju, E.; Bible, R.; Olmstead, M. M.; Maitra, K.; Fisher, A. J.; Balch, A. L.; Dorn, H. C. *Nature* **1999**, *401*, 55-57.

(2) Stevenson, S.; Lee, H. M.; Olmstead, M. M.; Kozikowski, C.; Stevenson, P.; Balch, A. L. *Chem. Eur. J.* **2002**, *8*, 4528-4535.

(3) Yamada, M.; Akasaka, T.; Nagase, S. *Accounts Chem. Res.* **2009**, *42*, in press (10.1021/ar900140n).

(4) Cai, T.; Xu, L.; Anderson, M. R.; Ge, Z.; Zuo, T.; Wang, X.; Olmstead, M. M.; Balch, A. L.; Gibson, H. W.; Dorn, H. C. *J. Am. Chem. Soc.* **2006**, *128*, 8581-8589.

(5) Zuo, T.; Beavers, C. M.; Duchamp, J. C.; Campbell, A.; Dorn, H. C.; Olmstead, M. M.; Balch, A. L. *J. Am. Chem. Soc.* **2007**, *129*, 2035-2043.

(6) Dunsch, L.; Yang, S. *Small* **2007**, *3*, 1298-1320.

(7) Qian, M.; Ong, S. V.; Khanna, S. N.; Knickelbein, M. B. *Phys. Rev. B* **2007**, *75*, 104424-1-6.

(8) Miyamoto, A.; Okimoto, H.; Shinohara, H.; Shibamoto, Y. *Eur. Radiol.* **2006**, *16*, 1050-1053.

(9) Stevenson, S.; Harich, K.; Yu, H.; Stephen, R. R.; Heaps, D.; Coumbe, C.; Phillips, J. P. *J. Am. Chem. Soc.* **2006**, *128*, 8829-8835.

(10) Stevenson, S.; Mackey, M. A.; Coumbe, C.; Phillips, J. P.; Elliott, B.; Echegoyen, L. *J. Am. Chem. Soc.* **2007**, *129*, 6072-6073.

(11) Elliott, B.; Yu, L.; Echegoyen, L. *J. Am. Chem. Soc.* **2005**, *127*, 10885-10888.

(12) Ge, Z. X.; Duchamp, J. C.; Cai, T.; Gibson, H. W.; Dorn, H. C. *J. Am. Chem. Soc.* **2005**, *127*, 16292-16298.

(13) Shustova, N. B.; Popov, A. A.; Mackey, M. A.; Coumbe, C. E.; Phillips, J. P.; Stevenson, S.; Strauss, S. H.; Boltalina, O. V. *J. Am. Chem. Soc.* **2007**, *129*, 11676-11677.

(14) Powell, W. H.; Cozzi, F.; Moss, G. P.; Thilgen, C.; Hwu, R. J. R.; Yerin, A. *Pure Appl. Chem.* **2002**, *74*, 629-695.

(15) Fowler, P. W.; Manolopoulous, D. E. *An Atlas of Fullerenes*; Dover: Mineola, NY, 2006.

(16) Shu, C.; Slebodnick, C.; Xu, L.; Champion, H.; Fuhrer, T.; Cai, T.; Reid, J. E.; Fu, W.; Harich, K.; Dorn, H. C.; Gibson, H. W. *J. Am. Chem. Soc.* **2008**, *130*, 17755-17760.

(17) Lee, H. M.; Olmstead, M. M.; Iezzi, E.; Duchamp, J. C.; Dorn, H. C.; Balch, A. L. *J. Am. Chem. Soc.* **2002**, *124*, 3494-3495.

(18) Cai, T.; Slebonick, C.; Xu, L.; Harich, K.; Glass, T. E.; Chancellor, C.; Fettinger, J. C.; Olmstead, M. M.; Balch, A. L.; Gibson, H. W.; Dorn, H. C. *J. Am. Chem. Soc.* **2006**, *128*, 6486-6492.

(19) Wakahara, T.; Iiduka, H.; Ikenaga, O.; Nakahodo, T.; Sakuraba, A.; Yoza, K.; Horn, E.; Mizorogi, N.; Nagase, S. *J. Am. Chem. Soc.* **2006**, *128*, 9919-9925.

(20) Hitchcock, P. B.; Avent, A. G.; Martsinovich, N.; Troshin, P. A.; Taylor, R. *Chem. Commun.* **2005**, 75-77.

(21) Cai, T.; Xu, L.; Gibson, H. W.; Dorn, H. C.; Chancellor, C. J.; Olmstead, M. M.; Balch, A. L. *J. Am. Chem. Soc.* **2007**, *129*, 10795-10800, and references therein.

(22) Hitchcock, P. B.; Avent, A. G.; Martisinovich, N.; Troshin, P. A.; Taylor, R. *Org. Lett.* **2005**, *7*, 1975-1978.

(23) Goryunkov, A. A.; Kuvychko, I. V.; Ioffe, I. N.; Dick, D. L.; Sidorov, L. N.; Strauss, S. H.; Boltalina, O. V. *J. Fluorine Chem.* **2003**, *124*, 61-64.

(24) Goryunkov, A. A.; Ioffe, I. N.; Kuvychko, I. V.; Yankova, T. S.; Markov, V. Y.; Streletskii, A. V.; Dick, D. L.; Sidorov, L. N.; Boltalina, O. V.; Strauss, S. H. *Fullerenes Nanotubes Carbon Nanostruct.* **2004**, *12*, 181-185.

(25) Dorozhkin, E. I.; Ignat'eva, D. V.; Tamm, N. B.; Goryunkov, A. A.; Khavrel, P. A.; Ioffe, I. N.; Popov, A. A.; Kuvychko, I. V.; Streletskiy, A. V.; Markov, V. Y.; Spandl, J.; Strauss, S. H.; Boltalina, O. V. *Chem. Eur. J.* **2006**, *12*, 3876-3889.

(26) Kareev, I. E.; Lebedkin, S. F.; Bubnov, V. P.; Yagubskii, E. B.; Ioffe, I. N.; Khavrel, P. A.; Kuvychko, I. V.; Strauss, S. H.; Boltalina, O. V. *Angew. Chem. Int. Ed.* **2005**, *44*, 1846-1849.

(27) Shustova, N. B.; Popov, A. A.; Newell, B. S.; Miller, S. M.; Anderson, O. P.; Seppelt, K.; Bolskar, R. D.; Boltalina, O. V.; Strauss, S. H. *Angew. Chem. Int. Ed.* **2007**, *46*, 4111-4114.

(28) Kareev, I. E.; Kuvychko, I. V.; Shustova, N. B.; Lebedkin, S. F.; Bubnov, V. P.; Anderson, O. P.; Popov, A. A.; Strauss, S. H.; Boltalina, O. V. *Angew. Chem. Int. Ed.* **2008**, *47*, 6204-6207.

(29) Kareev, I. E.; Popov, A. A.; Kuvychko, I. V.; Shustova, N. B.; Lebedkin, S. F.; Bubnov, V. P.; Anderson, O. P.; Seppelt, K.; Strauss, S. H.; Boltalina, O. V. *J. Am. Chem. Soc.* **2008**, *130*, 13471-13489.

(30) Kobayashi, K.; Sano, Y.; Nagase, S. *J. Comput. Chem.* **2001**, *22*, 1353-1358.

(31) Campanera, J. M.; Bo, C.; Olmstead, M. M.; Balch, A. L.; Poblet, J. M. *J. Phys. Chem. A* **2002**, *106*, 12356-12364.

(32) Alvarez, L.; Pichler, T.; Georgi, P.; Schwieger, T.; Peisert, H.; Dunsch, L.; Hu, Z.; Knupfer, M.; Fink, J.; Bressler, P.; Mast, M.; Golden, M. S. *Phys. Rev. B* **2002**, *66*, 035107/1-035107/7.

(33) Gan, L. H.; Yuan, R. *ChemPhysChem* **2006**, *7*, 1306-1310.

(34) Popov, A. A.; Dunsch, L. *J. Am. Chem. Soc.* **2008**, *130*, 17726-17742.

(35) Heine, T.; Vietze, K.; Siefert, G. *Magn. Reson. Chem.* **2004**, *42*, 199-201.

(36) Rodriguez-Fortea, A.; Campanera, J. M.; Cardona, C. M.; Echegoyen, L.; Poblet, J. M. *Angew. Chem. Int. Ed.* **2006**, *45*, 8176-8180.

(37) Cai, T.; Xu, L.; Shu, C.; Champion, H.; Reid, J. E.; Anklin, C.; Anderson, M. R.; Gibson, H. W.; Dorn, H. C. *J. Am. Chem. Soc.* **2008**, *130*, 2136-2137.

(38) Boltalina, O. V.; Popov, A. A.; Strauss, S. H. In *Strained Hydrocarbons. Beyond the van't Hoff and Le Bel Hypothesis*, Dodziuk, H., Wiley-VCH: Weinheim, 2009, pp 225-238.

(39) Hirsch, A.; Brettreich, M. *Fullerenes – Chemistry and Reactions*; Wiley-VCH: Weinheim, 2005.

(40) Matsuo, Y.; Fujita, T.; Nakamura, E. *Chem. Asian J.* **2007**, *2*, 948-955, and references therein.

(41) Sadow, A. D.; Tilley, T. D. *J. Am. Chem. Soc.* **2003**, *125*, 7971-7977.

(42) Yang, S.; Popov, A. A.; Dunsch, L. *Angew. Chem. Int. Ed.* **2007**, *46*, 1256-1259.

(43) Popov, A. A.; Dunsch, L. *Chem. Eur. J.* **2009**, *15*, 9707-9729.

(44) Popov, A. A.; Dunsch, L. *J. Am. Chem. Soc.* **2007**, *129*, 11835-11849.

(45) Goryunkov, A. A.; Markov, V. Y.; Ioffe, I. N.; Sidorov, L. N.; Bolskar, R. D.; Diener, M. D.; Kuvychko, I. V.; Strauss, S. H.; Boltalina, O. V. *Angew. Chem. Int. Ed.* **2004**, *43*, 997-1000.

(46) Troyanov, S. I.; Kemnitz, E. *Eur. J. Org. Chem.* **2003**, 3916-3919.

(47) Simeonov, K. S.; Amsharov, K. Y.; Jansen, M. *Chem. Eur. J.* **2008**, *14*, 9585-9590.

(48) Kemnitz, E.; Troyanov, S. I. *Angew. Chem. Int. Ed.* **2009**, *48*, 2584-2587.

(49) Haddon, R. C. *Science* **1993**, *261*, 1545-1550.

(50) Perdew, J. P.; Burke, K.; Ernzerhof, M. *Phys. Rev. Lett.* **1996**, *77*, 3865-3868.

(51) Laikov, D. N. *Chem. Phys. Lett.* **1997**, *281*, 151-156.

(52) Laikov, D. N.; Ustynyuk, Y. A. *Russ. Chem. Bull., Int. Ed.* **2004**, *54*, 820-826.

Table of Contents Graphic